Towards a Low Complexity Implementation of a Multi-H CPM Demodulator

TOWARDS A LOW COMPLEXITY IMPLEMENTATION OF A MULTI-H CPM DEMODULATOR

Arnaud Guéguen, David Auvray
Zodiac Data Systems SAS, 2 rue de Caen - F-14740 Bretteville l'Orgueilleuse - France
Arnaud.Gueguen and David.Auvray@zodiacaerospace.com
http://www.zodiacaerospace.com

ABSTRACT

Multi-h Continuous Phase Modulation (CPM) is a promising waveform for aeronautical telemetry because it is a compact spectrally efficient constant amplitude modulation. It has been selected as the Advanced Range Telemetry (ARTM) tier II waveform owing to these qualities. However, it is also a complicated waveform that has the reputation of suffering from complex demodulation processing and high sensitivity to transmission impairments and in particular synchronization aspects. In this paper we review a set of complexity reduction techniques that intend to bring this waveform into the domain of operational telemetry waveform, by allowing low complexity hardware implementation without sacrificing performance or robustness. Most techniques are adjustments of recent literature results, concerning both demodulation and synchronization. Computer simulation of a receiver implementing theses techniques shows negligible performance loss compared to optimal coherent demodulation with perfect synchronization. Hardware implementation confirms that nearly optimal performance can be achieved with hardware resource currently available in middle range FPGAs.

Keywords: Multi-h CPM, ARTM tier II, demodulation, synchronization, hardware implementation

I. INTRODUCTION

Aeronautical telemetry is likely to require more and more spectrally efficient waveforms as the radio spectrum is a scarce, expensive and shared resource, and because the amount of data to transmit is constantly increasing. Not only the selected waveforms shall have a constant modulus to put up with onboard amplifier constraints but also they shall require a rather low E_b/N_0 operating point and provide fast locking capabilities. Multi-h CPM has been selected as the ARTM tier II waveform [1] because it rather well fulfils these specifications [2]. However, the related optimal demodulator implementing maximum likelihood sequence estimation (MLSE) suffers from a large complexity that is hardly compatible with the hardware resources existing on nowadays programmable components. Therefore, much effort has been made in the research community to propose complexity reduction techniques that would allow reasonable

implementation complexity [3][4]. Besides, as traditional synchronization techniques based on signal constellation and eye diagram considerations fail to provide a workable solution in the case of multi-h CPM, some research has also been accomplished in this domain [6][7][8].

This paper aims at reviewing relevant complexity reduction and synchronization techniques to achieve a feasible implementation of an operational receiver. Most techniques require adjustments compared to what is proposed in the literature. However, these adjustments present too many details to be accurately described in the present paper. Instead, we highlight simulation results of the designed techniques, and give preliminary measurements of hardware prototyping based on these adjustments.

The paper is organized as follows: section II presents the signal model and section III recalls the optimal MLSE demodulation scheme. Then, section IV reviews complexity reduction techniques for demodulation based on recent literature results. Section V deals with synchronization aspects. Section VI focuses on implementation results and section VII draws conclusions.

II. SIGNAL MODEL

The transmitted ARTM tier II baseband signal is given by the following equations:

$$\begin{cases} s(t,\underline{\alpha}) = \sqrt{\dfrac{E}{T}} \exp\left(j2\pi\varphi(t,\underline{\alpha}) \right) \\ \varphi(t,\underline{\alpha}) = \displaystyle\sum_{i=0}^{\infty} h_i \alpha_i q(t-iT) \end{cases} \tag{1}$$

where E is the symbol energy, T is the symbol duration, $h_i \in \{4/16,5/16\}$ is the toggling modulation index, α_i are the modulated symbols taking values in the M=4 elements alphabet {-3,-1,1,3}, $\underline{\alpha}=\{\alpha_0,\alpha_1,\alpha_2,\ldots\}$ is the sequence of transmitted modulated symbols, $q(t)$ is the phase shaping function defined as:

$$\begin{cases} q(t) = \displaystyle\int_0^t f(\tau)\, d\tau \\ f(t) = \begin{cases} \dfrac{1}{2LT}\left(1-\cos\left(\dfrac{2\pi t}{LT}\right)\right) & t \in [0, LT] \\ 0 \quad t \notin [0, LT] \end{cases} \end{cases} \tag{2}$$

where L=3 is the support of the frequency shaping function $f(t)$.

The received baseband signal $r(t)$ is given by:

$$r(t) = \sqrt{\frac{E}{T}} \exp\left(j2\pi\varphi(t+\tau,\underline{\alpha}) \right) \exp\left(j\left(2\pi\Delta f t + \theta\right)\right) + \nu(t) \tag{3}$$

where τ, Δf and θ are respectively the delay error, the carrier offset and the carrier phase shift between the transmitter and the receiver. These impairments are considered as compensated except in the section dedicated to synchronization aspects. $\nu(t)$ is the Additive White Gaussian Noise (AWGN) with double sided power spectral density N_0.

III. OPTIMAL DEMODULATOR

The optimal receiver seeks the candidate sequence $\underline{\alpha}_{ML}$ such that (see e.g. [2]):

$$\underline{\alpha}_{ML} = \arg\max_{\underline{\alpha}} \left(\Pr\left(r(t) \middle| s\left(t, \underline{\alpha}\right) \right) \right) = \arg\max_{\underline{\alpha}} \left(\mathrm{Re}\left(\int_0^t r(u) s^*\left(u, \underline{\alpha}\right) \mathrm{d}u \right) \right) \tag{4}$$

This maximum likelihood sequence decoding is achieved in a recursive manner by the so-called Viterbi algorithm, which consists in finding the candidate sequence that maximizes the cumulated metrics λ_n recursively defined as:

$$\underbrace{\mathrm{Re}\left(\int_0^{(n+1)T} r(t) s^*\left(t, \underline{\alpha}\right) \mathrm{dt} \right)}_{\lambda_{n+1}} = \underbrace{\mathrm{Re}\left(\int_0^{nT} r(t) s^*\left(t, \underline{\alpha}\right) \mathrm{dt} \right)}_{\lambda_n} + \underbrace{\mathrm{Re}\left(\int_{nT}^{(n+1)T} r(t) s^*\left(t, \underline{\alpha}\right) \mathrm{dt} \right)}_{\text{Branch Metric}} \tag{5}$$

The branch metric is obtained using the fact that in the interval $[nT,(n+1)T]$ the signal $s(t,\underline{\alpha})$ can be expressed as:

$$s\left(t, \underline{\alpha}\right) = \exp\left(j\left(\theta_{n-L} + \theta\left(t - nT, \underline{\alpha}_n\right) \right) \right) \tag{6}$$

where

$$\theta_{n-L} = \pi \sum_{i=0}^{n-L} h_i \alpha_i \tag{7}$$

is a cumulated phase rotation term at instant $t=nT$, having $p=32$ possible values and

$$\theta\left(t - nT, \underline{\alpha}_n\right) = 2\pi \sum_{i=n-L+1}^{n} h_i \alpha_i q\left(t - iT\right) \tag{8}$$

is the phase trajectory in the interval $[nT,(n+1)T]$, and $\underline{\alpha}_n = \{\alpha_{n-L+1}, \ldots, \alpha_n\}$ is the length L modulated symbols sequence determining the phase trajectory in $[nT,(n+1)T]$. Hence, the branch metric is given by:

$$BM = \mathrm{Re}\left(e^{-j\theta_{n-L}} \int_{nT}^{(n+1)T} r(t) e^{-j\theta\left(t - nT, \underline{\alpha}_n\right)} \mathrm{d}t \right) \tag{9}$$

Equations (6), (7) and (8) give the size of the Viterbi decoder trellis. Indeed, the phase value at $t=nT$ is fully defined by $\{\theta_{n-L},\alpha_{n-L+1},\ldots,\alpha_{n-1}\}$, which gives pM^{L-1}=512 trellis states. Besides, the phase trajectories in $[nT,(n+1)T]$ are fully defined by $\{\theta_{n-L},\alpha_{n-L+1},\ldots,\alpha_{n}\}$, which gives pM^{L}=2048 branches (M=4 branches leaving each state).

Figure 1 illustrates the corresponding optimal demodulator architecture. The $N=M^L$=64 complex filters are matched to the 64 possible phase trajectories $\theta(t,\underline{\alpha}_n)$ in a symbol time interval. This architecture leads to 256 real filters and 2048 branch metric computations per symbol interval.

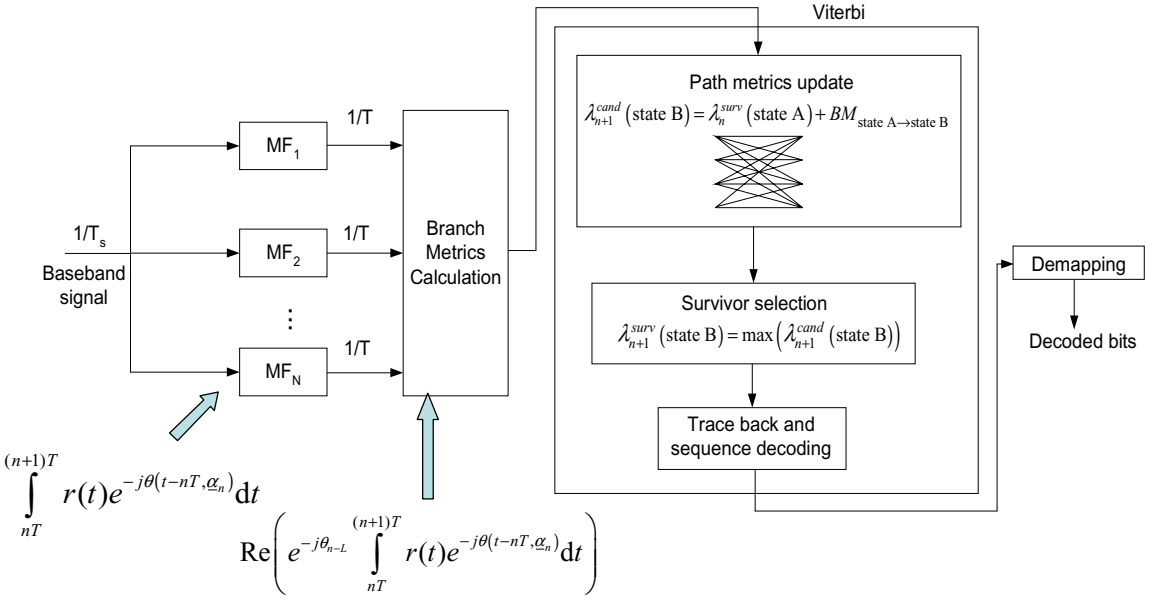

Figure 1 : simplified architecture of optimal demodulator

Considering an implementation with 4 samples per symbol, a baud rate of $B=1/T$=25MBd, a 100MHz internal clock, this demodulation scheme requires a total of 1280 multipliers, which is still a lot for commonly available FPGAs, all the more so as a similar amount of hardware is required for synchronization.

The simulated Bit Error Rate (BER) performance of the optimal receiver is represented on the curve "Optimal MLSE" of Figure 4. It is consistent with what is predicted by the union bound [3].

IV. LOW COMPLEXITY DEMODULATOR

1. Reduced dimension representation

The first technique allows a drastic reduction in the number of matched filters at the expense of small performance degradation. It is based on reduced dimension representation of the transmitted signal, similarly to what has been proposed in [4].

The candidate transmitted signal portion of $s(t,\underline{\alpha})$ in $[nT,(n+1)T]$ expressed in (6) can be written as a linear combination of elementary functions:

$$s(t,\underline{\alpha})_{t\in[nT,(n+1)T]} = e^{j\theta_{n-L}}\sum_{j=1}^{M^L} C_j(\underline{\alpha}_n)\varphi_j(t-nT) = e^{j\theta_{n-L}}\mathbf{C}(\underline{\alpha}_n)\mathbf{\Phi}(t-nT) \quad (10)$$

where $\{\varphi_j(t)=\exp(j2\pi\theta(t,\underline{\alpha}_n))\}_{j=1..64}$ is the ensemble of all M^L possible signal portions related to the corresponding phase trajectories, $C_j(\underline{\alpha}_n)$ is a scalar equal to 1 when the index j of $\varphi_j(t)$ corresponds to the symbol sequence $\underline{\alpha}_n$, and equal to 0 otherwise. $\mathbf{C}(\underline{\alpha}_n)$ is a M^L line vector made of all $C_j(\underline{\alpha}_n)$, $\mathbf{\Phi}(t\text{-}nT)$ is a M^L column vector made of all functions $\varphi_j(t\text{-}nT)$.

The ensemble $\{\varphi_j(t)=\exp(j2\pi\theta(t,\underline{\alpha}_n))\}_{j=1..64}$ is represented on Figure 2.

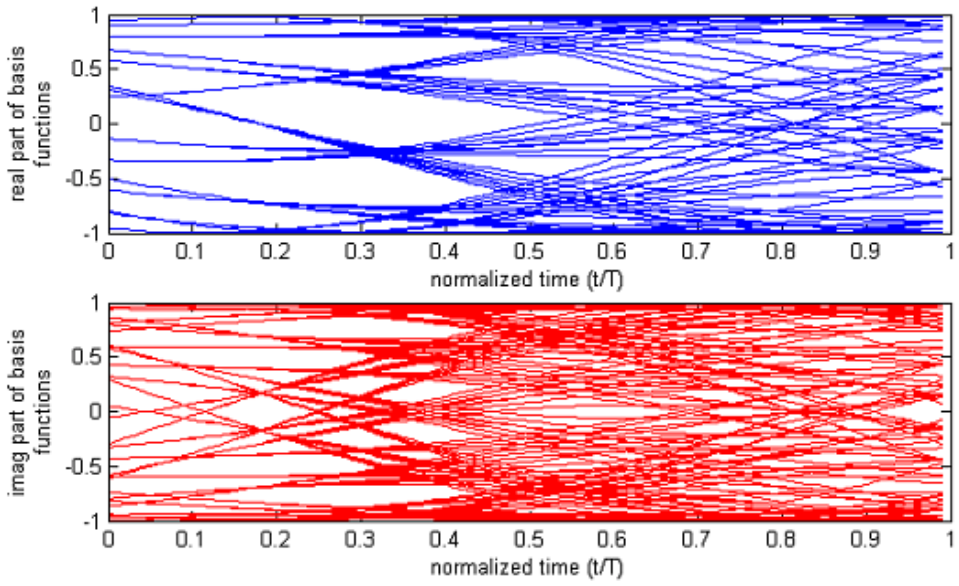

Figure 2 : real and imaginary parts of all possible signal portions in [0,T]

Moving to discrete time representation with K samples per symbol duration, $\mathbf{\Phi}(t\text{-}nT)$ becomes a M^LxK matrix $\mathbf{\Phi}$ with a rank upper bounded by $\min(M^L,K)$.

From the singular value decomposition of $\mathbf{\Phi}$, it appears that more than 99% of the signal energy is contained in the 2 dominant eigenmodes, which are real valued. Hence, matrix $\mathbf{\Phi}$ can be approximated using reduced dimension representation as:

$$\mathbf{\Phi} = \mathbf{U}\mathbf{\Lambda}\mathbf{V}^H \approx \mathbf{U}'\mathbf{\Lambda}'\mathbf{V}'^H \quad (11)$$

where $\mathbf{U}$ is a M^LxM^L unitary matrix, $\mathbf{\Lambda}$ is a M^LxK diagonal matrix, $\mathbf{V}$ is a KxK unitary matrix, $\mathbf{U'}$ is a M^LxK' matrix made of the $K'<K$ vectors of $\mathbf{U}$ related to the K' main singular values, $\mathbf{\Lambda'}$ is a

*K'*x*K'* diagonal matrix made of the *K'* main singular values, **V'** is a *K'*x*K* matrix made of the *K'* vectors of **V** related to the *K'* main singular values.

This representation of **Φ** allows reducing the number of matched filters to the number *K'* of selected main singular values. Using the two main eigenmodes, and hence only two real matched filters instead of 64 original complex matched filters in the reference optimal receiver, it appears from simulation that the performance degradation is less than 0.1 dB with respect to the optimal receiver described in previous section, see the curve "MLSE 2MF" of Figure 4.

2. State Space Partitioning (SSP)

The second main simplification consists in reducing the trellis size by partitioning the signal state space, similarly to what is presented in [3][5].

As explained in [5], two states of a trellis can be grouped together into the same part of the state space partition with reduced performance impact, provided that two paths emerging from a given state and arriving in these two states are separated by an Euclidean distance that is larger than the intrinsic code Euclidean distance. Such a configuration is illustrated on Figure 3.

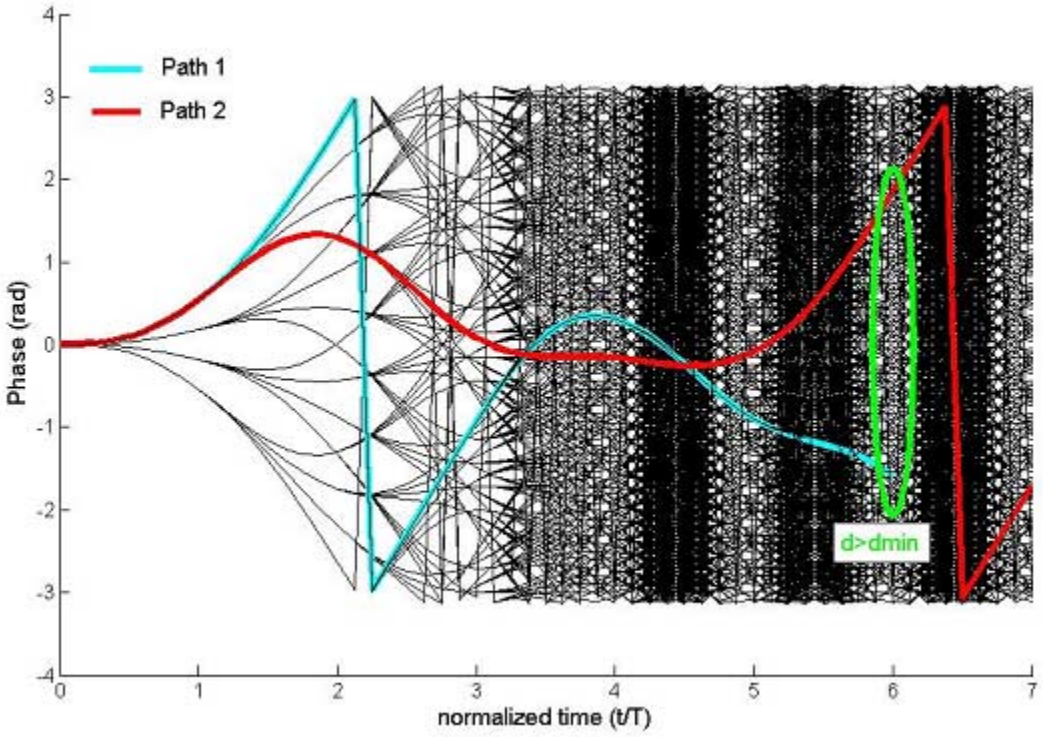

Figure 3 : two paths arriving in different states of a same part

Applying an exhaustive search algorithm on the trellis makes it possible to identify a partition of $\{\theta_{n-L},\alpha_{n-L+1},\ldots,\alpha_{n-1}\}$, that reduces the state space as much as possible without sacrificing the BER performance. A 64 parts partition has been identified that induces negligible BER degradation, as shown on the curve "MLSE 2MF SSP" of Figure 4.

3. Performance evaluation

The performances are evaluated with AWGN channel.

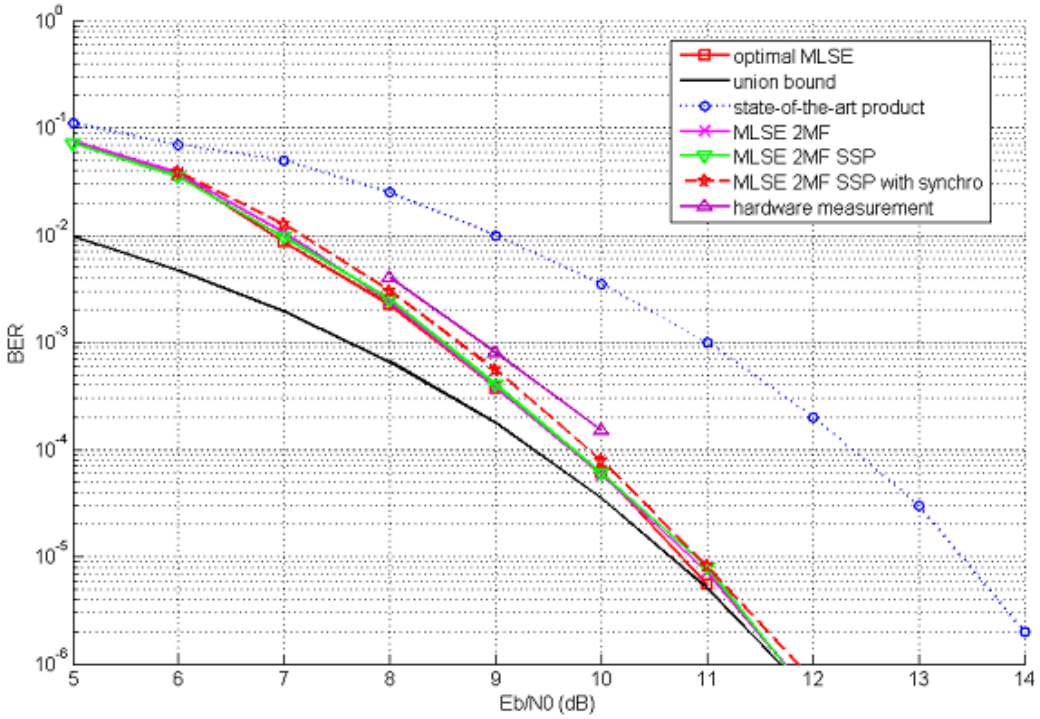

Figure 4 : simulated and measured BER performance (state-of-the-art product, see [9])

V. SYNCHRONIZATION ASPECTS

Synchronization is as critical as demodulator complexity to achieve operational multi-h CPM reception.

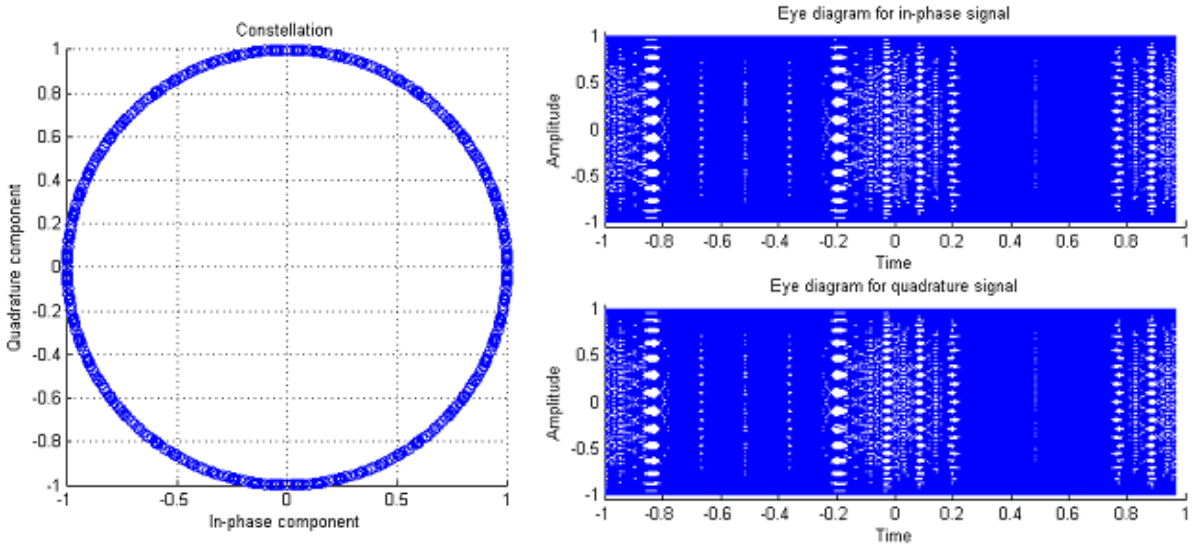

Figure 5 : constellation and eye diagram of a multi-h CPM signal (no distortion)

Indeed, four levels of synchronization are needed to perform coherent multi-h CPM demodulation: carrier frequency, carrier phase, timing and index. These synchronization operations must be fast, accurate and robust. Besides, considering the signal characteristics (see Figure 5), "traditional" techniques based on signal constellation and eye diagram can obviously not be applied.

1. Frequency and phase synchronization

Frequency and phase synchronizations are crucial for coherent demodulation. We designed a robust and low complexity frequency synchronization by deriving a frequency error estimator based on [6]:

$$\hat{\Delta f} = \arg\max_{\Delta f} \underbrace{E_{\underline{\alpha},\theta,\tau}\left(\Pr\left(r(t)\middle|s\left(t,\underline{\alpha},\Delta f,\theta,\tau\right)\right)\right)}_{\lambda\left(\Delta f\right)} \tag{12}$$

where $\Pr(r(t)|s(t,\underline{\alpha},\Delta f,\theta,\tau))$ is the probability density of the received signal r(t), conditioned on a transmitted signal with carrier frequency error Δf, carrier phase error θ, timing error τ and carrying a symbol sequence $\underline{\alpha}$.

The metric $\lambda(\Delta f)$ is obtained by marginalizing this conditional probability with respect to $\underline{\alpha}, \theta$ and τ. Its derivative with respect to Δf can then be estimated as discussed in [6]. When combined with dimension reduction techniques similar to section IV.1, we obtain a derivative estimate that features very low complexity. The derivative is then used in a loop that implements a gradient search algorithm to converge towards the expected value of Δf:

$$\hat{\Delta f} = \hat{\Delta f} - \gamma \frac{d\lambda\left(\Delta f\right)}{d\Delta f} \tag{13}$$

where γ is a loop parameter that is chosen in order to trade-off residual estimation error and convergence speed. We optimised this synchronization algorithm so that only few thousands of symbols are required to achieve reasonable residual unbiased carrier error.

In order to coherently demodulate the signal, accurate phase synchronization must be implemented. As suggested in [7], decision-directed phase estimation techniques provide an appropriate solution.

2. Timing synchronization

Timing synchronization must both correct baud rate errors and activate sampling at the right instants in the symbol time interval.

Reference [8] presents a robust non decision-aided timing acquisition technique that is appropriate for CPM. The estimator is given by:

$$\hat{\tau} = \arg\max_{\tau} \underbrace{E_{\underline{\alpha},\theta}\left(\Pr\left(r(t)\middle|s\left(t,\underline{\alpha},\theta,\tau\right)\right)\right)}_{\lambda(\tau)} \tag{14}$$

It needs some modifications in order to take into account the index alternation of multi-h CPM. These modifications also naturally provide index synchronization.

The designed frequency and timing synchronization techniques were validated through computer simulations. The BER performance degradation due to residual synchronization errors is in the order of 0.2 dB, as can be seen on the curve "MLSE 2MF SSP with synchro" of Figure 4. The reported BER performances are measured after a synchronization lock is detected. The impairments set for these simulations are: a frequency offset of 10% of the baud rate $1/T$, a random timing offset in $[0, 2T]$, and a baud rate error of 50 ppm. The minimum Eb/N_0 required for locking is 4 dB.

VI. IMPLEMENTATION RESULTS

Table 1 summarizes preliminary prototyping results of a stand-alone baseband mutli-h CPM demodulator without synchronization logic, based on the techniques reviewed in the previous sections for various hardware targets.

Target	Virtex2 XCV6000FF1152-4	Virtex4LX80FF1148-10	Virtex5vsx95t-2ff1136
Number of Mult18x18s	68 (47%)	68 (85%)	68 (10%)
Number LUTs	42298 (62%)	47662 (66%)	36768 (62%)
Number of RAMB16s	76 (52%)	75 (37%)	70 (28%)
Number of occupied slices	24575 (72%)	28244 (76%)	12058 (81%)
Rate Max	25 Mbps	25 Mbps	40 Mbps

Table 1 : implementation summary for various FPGA targets

Performance evaluation of the corresponding implementation is reported on Figure 4. A performance loss of 0.5 dB is observed compared to the optimal MLSE.

VII. CONCLUSION

This paper gives an overview of complexity reduction and synchronization techniques for multi-h CPM reception. Reduced dimension description of the multi-h CPM signal provides a reduction in the number of matched filters by a factor 64 compared to optimal processing, while state-space partitioning makes it possible to reduce the number of trellis states by a factor 8. Non data-aided frequency and timing synchronization combined with decision-oriented phase synchronization enable accurate and robust synchronization that makes coherent demodulation feasible at an

affordable hardware cost. We foresee deploying these techniques into a rather low complexity hardware implementation of an operational ARTM tier II compliant coherent receiver performing within 0.5 dB from the optimal coherent MLSE decoder, without sacrificing signal acquisition time.

VIII. REFERENCES

[1] Range Commanders Council Telemetry Group, Range Commanders Council, White Sands Missile Range, New Mexico, IRIG Standard 106-04: Telemetry Standards, 2004.

[2] Geoghegan M.S., “Description and Performance Results for the Advanced Range Telemetry (ARTM) Tier II Waveform”, Proceedings of the International Telemetering Conference, October 2000.

[3] E. Perrins and M. Rice, "Reduced Complexity Detectors for Multi-h CPM in Aeronautical Telemetry", IEEE Transactions on Aerospace and Electronic Systems, vol. 43, no. 1, pp. 286-300, January 2007.

[4] Moqvist, P., and Aulin, T. "Orthogonalization by principal components applied to CPM. IEEE Transactions on Communications", 51 (Nov. 2003), 1838—1845.

[5] Larsson, T. "A state-space partitioning approach to trellis decoding". Ph.D. dissertation, Chalmers University of Technology, Göteborg, Sweden, Dec. 1991.

[6] Andrea A.N., Ginesi A., Mengali, U., "Frequency detectors for CPM signals", IEEE Transactions on Communications Volume 43, Issue 234, Feb/Mar/Apr 1995 Page(s):1828 – 1837.

[7] Giulio Colavolpe and Riccardo Raheli, "Reduced-complexity detection and phase synchronization of CPM signals", IEEE Transactions on Communications, 45, September 1997.

[8] D'Andrea, U. Mengali, M. Morelli, "Symbol Timing Estimation with CPM Modulation", IEEE Transactions on Communications, Vol. 44, pp. 1362-1371, 1996.

[9] http://www.quasonix.com/uploads/qsx_demodulator_ds_web.pdf